Acoustic anisotropy of piezoelectric $LiNbO_3$ crystals and its application in integrated acousto-optical tunable filters*

WEN Chuan-jing * * **and YANG Ji-sheng**
Department of Applied Physics, Tianjin University, Tianjin 300072, *China*

(Received 20 Jan. 2005)

We use Jones's matrix method and the global optimal method to investigate the propagation characteristic of surface acoustic wave(SAW) for *X*-cut single crystal Lithium Niobate($LiNbO_3$). As an application, a novel integrated acousto-optical filter, which allows to minimize the dimension of AO cells and suppress side-lobes, was designed on the base of $LiNbO_3$ crystal.

CLC number: O734; TN713 **Document code**: A **Article ID**: 1673-1905(2005)01-0001-04

Integrated Acousto-Optical Tunable Filters(IAOTF) have demonstrated wide application in various fields of laser technology, spectroscopy, optoelectronics and optical signal processing as well as wavelength division multiplexed(WDM) networks. IAOTF employ the interaction between surface acoustic wave and optic beams.

Because of its unique acousto-optic, electro-optic, photoelastic, piezoelectric and nonlinear properties, lithium niobate($LiNbO_3$) is widely used in a variety of integrated and active acousto-optic devices. The design of such devices and the analysis of the propagation characteristics of acoustic waves require accurate values of the $LiNbO_3$ acoustic physical constants. As a crystal belonging to the class 3 m of the trigonal system, $LiNbO_3$ has 12 acoustic physical constants comprising six elastic constants (c_{11}, c_{12}, c_{13}, c_{14}, c_{33} and c_{44}), four piezoelectric stress constants (e_{15}, e_{22}, e_{31} and e_{33}), and two dielectric constants (ε_{11} and ε_{33}). And the new constant data from G. Kovacs's work[1] is used.

The *X*-*Y*(*X* cut, *Y* propagation) orientation of $LiNbO_3$ has perhaps been avoided because acoustic anisotropy causes a y-directed acoustic beam to walk off at an appreciable angle from a y-propagating optical wave limiting the acousto-optic interaction length. This putative limitation can be easily circumvented and there are significant advantages to use the *X*-cut orientation over the popular *Y*-cut, namely an enhanced photoelastic effect as well as a stronger piezoelectric coupling for SAW excitation.

In the present paper, the more detailed fundamental properties of the surface acoustic waves on $LiNbO_3$ are described. In Section 2, the calculation procedure of the surface acoustic wave is briefly reviewed using J. J. Campbell and W. R. Jones's method[2] and the global optimal method[3], and the practical selection procedure for the roots of an equation of motion is presented for $LiNbO_3$. In Section 3, a novel quasi-collinear IAOTF is investigated theoretically and experimentally. Finally, the conclusions will be presented in Section 4.

A rectangular coordinate system (Fig. 1) is chosen with X_3 axis normal to the crystal surface and X_1 axis in the direction of propagation. Arbitrary orientations of the crystal surface with respect to the crystal axes (X, Y, Z) are considered. This is accomplished by means of a coordinate rotation through the Euler angles from the crystal axes (X, Y, Z) to the desired X_1 X_2 X_3 coordinate system. The matrix defining such a rotation is given by[4]

$$V = \begin{bmatrix} \cos\varphi\cos\Psi - \cos\theta\sin\varphi\sin\Psi & \sin\varphi\cos\Psi + \cos\theta\cos\varphi\sin\Psi & \sin\theta\sin\varphi \\ -\cos\varphi\sin\Psi - \cos\theta\sin\varphi\cos\Psi & -\sin\varphi\sin\Psi + \cos\theta\cos\varphi\cos\Psi & -\sin\theta\cos\varphi \\ \sin\theta\sin\Psi & \sin\theta\cos\Psi & \cos\theta \end{bmatrix} \quad (1)$$

where φ, θ, Ψ are the Euler angles. The two first Euler angles describe the orientation of the surface (crystal cut), while the third angle specifies the propagation direction of the wave along this surface.

Since the X_1 X_2 X_3 coordinate system is relative to the crystal surface and direction of propagation, the form of the differential equations for the mechanical displacement and electric potential in this coordinate system is independent of the surface under consideration. All the tensor components of the constitutive constants should be recalculated using the Euler angles (φ, θ, Ψ) for each orientation. Only the values of the coefficients change with the surface orientation relative to the crystal axes. This is also true of the boundary conditions. Different cuts are thus distinguished only through the transformed tensor quantities involved in coefficient of the differential

* Supported by the National Natural Science Foundation of China (No. 60478036)

* * E-mail: wenchuanjing@hotmail.com

operators,

$$C'_{ijkl}u_{k,li} + e'_{kij}\varphi_{,ki} = \rho\ddot{u}_j \quad (2)$$

$$e'_{ikl}u_{k,li} - \varepsilon'_{ik}\varphi_{,ki} = 0 \quad (3)$$

$$\nabla^2\varphi = 0 \quad (4)$$

where the primed quantities refer to a rotated coordinate system, and unprimed correspond to the coincidence of the X_1 X_2 X_3 coordinate system and the crystal axes, i.

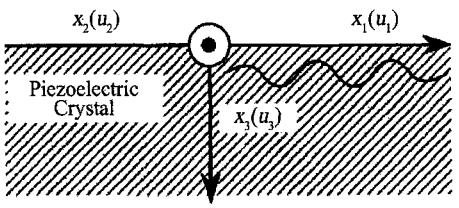

Fig. 1 The coordinate systems used in the calculation

e., when V is the identity matrix. As indicated above the surface waves under consideration are assumed to be traveling in the X_1 direction along a surface whose normal is in the X_3 direction. The displacement and potential are considered to be independent of the X_2 coordinate. Consequently, traveling-wave solutions of the form:

$$u_i = \beta_i \exp(-\alpha\omega x_3/v_s)\exp[\mathrm{i}\,\omega(t - x_1/v_s)] \quad (i = 1,2,3) \quad (5)$$

$$\varphi = \beta_4 \exp(-\alpha\omega x_3/v_s)\exp[\mathrm{i}\,\omega(t - x_1/v_s)] \quad (6)$$

are sought. When these surface wavefronts (as identified by an exponential decay into the crystal) are substituted into the differential equations (2), (3), (4) for $X_3 > 0$ a linear homogenous system of four equations in the unknown (β_1, β_2, β_3, β_4) produces. The determinant of these equations must be zero in order that nontrivial solutions exist. Evaluation of the above determinant results in an eight-order polynomial in α of the form:

$$A_8\alpha^8 + \mathrm{i}A_7\alpha^7 + A_6\alpha^6 + \mathrm{i}A_5\alpha^5 + A_4\alpha^4 + \mathrm{i}A_3\alpha^3 + A_2\alpha^2 + \mathrm{i}A_1\alpha + A_0 = 0 \quad (7)$$

where the coefficient An, are purely real and a particular value of v_s has been assumed. Since the fields must be bounded, or go to zero as $x_3 \to \infty$, only the roots with nonnegative real parts are allowed. In addition, these roots either are imaginary or occur in pairs with positive and negative real parts. In general, roots occur such that four with positive real parts can be selected. So the total fields (mechanical displacement and potential) may now be expressed as a linear combination of the fields associated with the admissible values of α. For $x_3 > 0$

$$u_i = \sum_{l=1}^{4} B^{(l)}\beta_i^{(l)} \exp(-\alpha^{(l)}\omega x_3/v_s) \times \exp[\mathrm{i}\omega(t - x_1/v_s)](i = 1,2,3) \quad (8)$$

$$\varphi = \sum_{l=1}^{4} B^{(l)}\beta_4^{(l)} \exp(-\alpha^{(l)}\omega x_3/v_s) \times \exp \times [\mathrm{i}\,\omega(t - x_1/v_s)] \quad (9)$$

Mechanical and electrical boundary condition must also be satisfied by substituting the waveform into the appropriate expression for these conditions. The boundary conditions for the elastic quantities are

$$T_{3j}\big|_{x_3=0} = 0 \quad (10)$$

and the boundary condition for the electric quantities,

$$D_3\big|_{x_3=0} = -\varepsilon_0 \frac{\partial\varphi}{\partial x_3}\bigg| \quad (11)$$

for free surface

$$\varphi\big|_{x_3=0} = 0 \quad (12)$$

for metallized surface.

This yeilds a set of homogenous equations. The transcendental equation obtained by setting the determinant of the matrix of coefficient of this system equal to zero determines the surface-wave velocities.

A computer program was written to solve this problem. Substituting the elastic constants, piezoelectric constants and dielectric constants of $LiNbO_3$ into the program with proper transformation matrices, the SAW velocity curve of X-cut was obtained (Fig. 2). And we know that there is about 4° walk-off for the X-Y orientation.

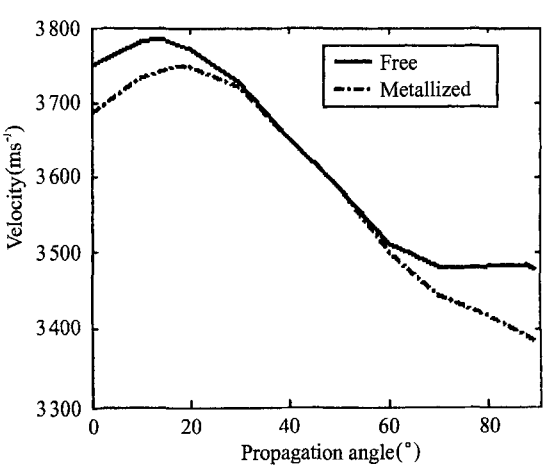

Fig. 2 Propagation characteristics of SAW in X-cut $LiNbO_3$ (propagation angle calculating from y axis)

It should be noted that the efficiency of the search for the minimum of the target function depends on the proper choice of the search region boundaries. A narrower search region ensures a faster and more reliable extremum search. However, if the search region is too narrow, the solution may lie beyond its boundaries and will not be found. A broad search region requires a great number of nodes of the calculation mesh for seeking the narrow maximum and, therefore, more computer time (but not memory for the method used). The search region boundaries are chosen on the basis of some auxiliary information, for example, from the preliminary calculated velocities of the volume waves for the given orientation. For example, we know that the SAW velocity must be smaller than the velocity of a slow quasishear volume wave, the velocity of the pseudosurface acoustic wave must lie between the velocities of the slow and fast quasishear volume waves, and the velocity of the high-velocity pseudosurface acoustic wave must be close (sometimes not very close) to the velocity of the quasi-longitudinal volume wave.

This information allows us to specify the search region boundaries.

SAW controlled integrated optical TE-TM mode converters are the core of IAOTF in WDM fiber optic communication systems.

IAOTF are attractive as they offer broad tuning ranges, fast tuning speed, non-multi-orders diffraction and non-moving parts. *X-Y* interaction geometry on $LiNbO_3$ was proposed, which results in a significant reduction of the power requirement. The disadvantage in a collinear IAOTF configuration is that although the direction of light propagation and the acoustic phase velocity are by definition collinear, the resulting acoustic group velocity follows a slightly different angle. To compensate for the walk-off of the SAW, the quasi-collinear TE/TM mode converter was fabricated by use of an angular offset between the acoustic and optical waveguides. Wide-angular quasi-collinear filters possess much better optical throughput because of wide linear and angular optical apertures as well as low RF driving power levels. Our design (Fig. 3) has simple structure configuration and fabrication technique as well as good performance of suppressing sidelobes.

First the optical waveguide is fabricated by diffusion of Ti-stripes for 10 hours at 1050 ℃. Then the interdigital transducer(IDT) consisting 10 pairs of fingers with period of 20.8 μm is deposited to allow the excitation of SAW. Up to now, most of the SAW devices utilize surface wave beam. To confine the acoustic wave field, an acostical waveguide is usually applied.

The acoustical waveguide is fabricated by SiO_2/In_2O_3 thin film. It is a good substitution of Ti-indiffusion. The film offers as lightly modrate reduction in SAW phase

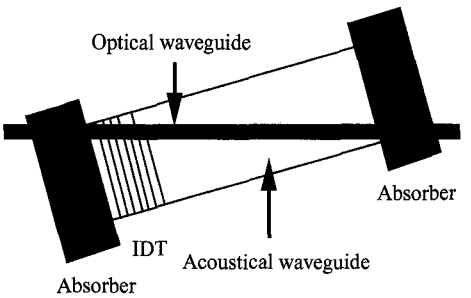

Fig. 3 The structure of the integrated quasi-collinear coupled IAOTF mode converter

velocity in the guiding region. Fig. 4 presents the velocity difference modeled for SiO_2/In_2O_3 using E. L. Adler's theory[5] and J. S. Yang's work[6]. Then a film of SiO_2/InO_3 is deposited as acoustical waveguide. And the acousto-optic interaction is apodised through use of an angular offset between the acoustic and optical waveguides to ensure a constant acoustic phase along the optical path and it is more likely to provide an optimized filter response. The acousto-optical interaction length is 25 mm and the angle between acoustical and optical waveguides is 0.42° (Fig. 3)[7]. The experimental results have been measured (Fig. 5). In our design the transducer was not optimized to compensate for the acoustic walk-off. A slight rotation of the transducer has been shown to improve the efficiency of launching acoustic waves in diffused SAW guides, and it is expected that a similar improvement could result when applied to the strip-loaded guide under investigation.

We have designed and investigated the properties of quasi-collinear AOTF based on the media with a strong

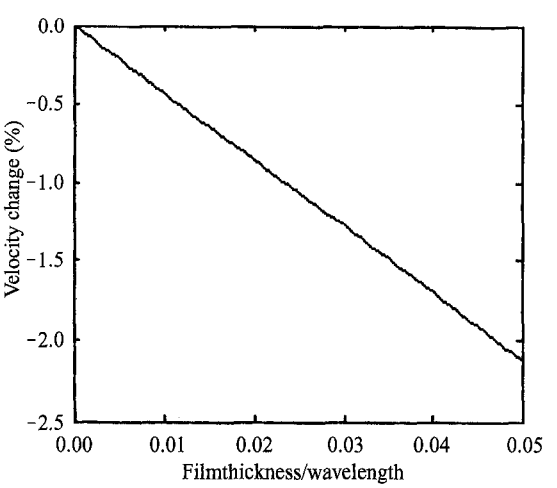

Fig. 4 SAW velocity vs thickness of the for SiO_2/InO_3 film

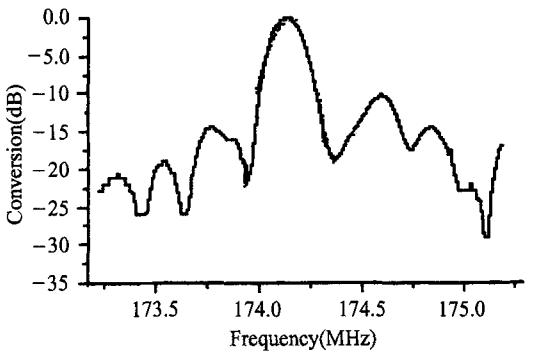

Fig. 5 The conversion characteristics of the mode converter: TE to TM

acoustic anisotropy $LiNbO_3$ single crystal. A novel integrated geometry of quasi-collinear filter designed on the base of $LiNbO_3$ crystal is proposed. We also fabricated the experimental prototype of quasi-collinear AOTF mode converter. At designing of AOTF prototype, we have used the quasi-collinear integrated that allows to minimize the dimensions of AO cells and suppress side-lobes.

References

[1] Kovacs G., Anhorn M., and Engan H. E. *Proc IEEE Ultrason Symp*, (1990), 435.

[2] Campbell J. J. and Jones W. R. *IEEE Sonics Ultrasonics*, **su-15** (1968), 209.

[3] Yu M., Dvoesherstov, Cherednik V. I., and Chirimanov A. P. *Radiophysics and Quantum Electronics*, **43** (2000), 719.

[4] Goldstein H. and Classic Mechanics. Addison Wesley, New York: 1950.

[5] Alder E. L., Slaboszewicz J. K., and Farnell G. W. *IEEE Trans Ultrason Ferroelectr Freq Control*, **37** (1990), 215.

[6] Yang J. S., Hao Y. C., and Zhang H. B. *Proceedings of SPIE*, **4603** (2001), 73.

[7] Hu H. Z., Lin H. Y., and Yang J. S. *Optics Communications*, **208** (2002), 79.